INTERSECTII
INTERSECTIONS
http://www.intersections.ro

Parametric Study on the Structural Behaviour of AAC-Reinforced Concrete Hybrid Lintels

Dorina-Nicolina Isopescu, Cristina Lanivschi and Oana Neculai
Department of Civil and Industrial Engineering, Gheorghe Asachi University, Iasi, 700050, Romania

Summary

The paper contains a numerical analysis on AAC-RC hybrid lintels structural behaviour, considering a variation in components heights, for the same overall cross-sectional area. The parametric study focused on the evaluation of deflections and stresses in lintel components and at AAC-concrete interface, for two types of contact behaviours: perfectly bonded and frictional.

Keywords: hybrid lintels, AAC, contact behaviour, interface, frictional.

1. INTRODUCTION

There is a number of scientific papers on structural elements obtained by combining aerated autoclaved concrete (AAC) with reinforced concrete (RC), but the research on the AAC-RC interface is limited and parametric studies on the ratio between the two components are scarce, [1, 2, 3, 4].

The current paper contains part of a research programme requested by the producer of these hybrid AAC-RC lintels, with the purpose to evaluate the structural behaviour of these elements, [5].

The research presented hereinafter represents a parametric numerical analysis on hybrid lintels made of an upper layer of RC and a lower layer of AAC, considering a constant overall cross-sectional area for the element, but varying the height of each component.

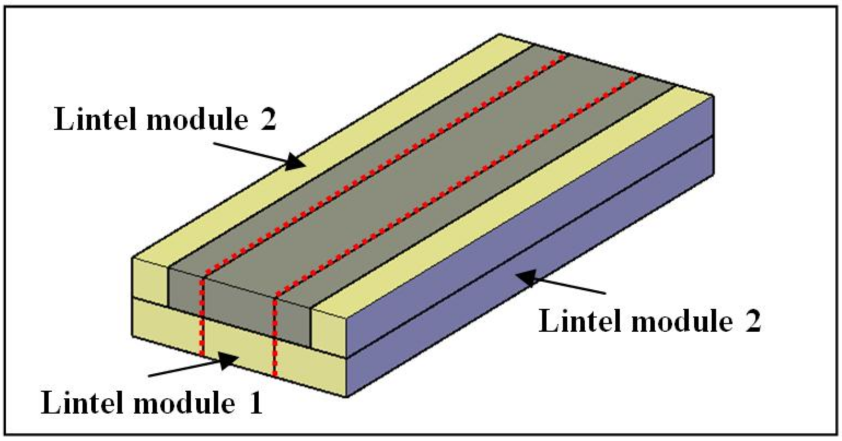

Figure1. Example of compound element made of lintel modules

The analysed lintels have 0.1 x 0.1 m cross-sections and represent part of a larger compound structural element, made of two types of lintel modules, as presented in Fig.1.The main advantage in using lintel modules is that there are theoretically no limits in the compound lintels widths, their dimensions being modulated to 0.1 m. Lintel module 1 is the focus of the current paper.

The purpose of the parametric study was to evaluate stresses in all components of hybrid lintel module 1 and their maximum deflections, for two different approaches on contact behaviour, in order to draw conclusions regarding the influence of the concrete-reinforcement and concrete-AAC bonds for the structural response of the lintel.

The final aim of the analysis was to determine the most advantageous configuration for the lintel cross-section from economical, strength and stiffness points of view.

2. FINITE ELEMENT ANALYSIS OF THE HYBRID LINTELS

The finite element analysis was performed using ANSYS Workbench V15.0, starting from a reference model that was validated in a previous research stage, when the simulation results were confirmed by analytical calculus, [6, 7].

The models consisted of an upper layer made of C20/25 concrete reinforced with longitudinal S500H steel bars and triangular stirrups and a lower AAC layer.

Two different approaches were analysed, related to RC-AAC contact behaviour. An “ideal” model was defined by considering perfectly bonded RC-AAC contact behaviour. Considering that in reality such compatibility between components cannot be achieved, a different scenario was used.

ISSN 1582-3024

To describe the weak bond between the two components, a Coulomb friction model was introduced by assigning a friction coefficient of only 0.001. This value was chosen to be very small, considering that a real bond between concrete and AAC is not possible due to the fabrication process of the lintels.

2.1. Geometry and material properties

The hybrid lintels cross-section overall dimensions are 0.1 x 0.1 m and length of 2.75 m, consisting of three components: AAC blocks with standardized compressive strength of f_b = 3.50 MPa, C20/25 strength class concrete and S500H steel reinforcement, consisting of three longitudinal bars of Ø4 mm diameter and triangular stirrups of Ø3 mm diameter, spaced at 15 cm lengthwise.

There are 11 lintel models, with the same length and cross-section dimensions, but with different heights for the AAC and RC layers, varying from 0.0 cm to 10 cm, using a step of 0.5 cm, as shown Table 1. For a more intuitive understanding of the models' names, the dimensions are measured in cm.

Table 1. Definition of models and component layers heights

Lintel model	Model name	AAC layer height hAAC, [cm]	RC layer height hRC, [cm]
1	M0.0	0.0	10
2	M0.5	0.5	9.5
3	M1.0	1.0	9.0
4	M1.5	1.5	8.5
5	M2.0	2.0	8.0
6	M2.5	2.5	7.5
7	M3.0	3.0	7.0
8	M3.5	3.5	6.5
9	M4.0	4.0	6.0
10	M4.5	4.5	5.5
11	M5.0	5.0	5.0

The models are denoted with an initial M for "model" followed by the thickness of AAC layer, in cm, and by a superscript "b" – for bonded and "f" – for frictional, M $h_{AAC}^{b/f}$, as shown Figure 2.

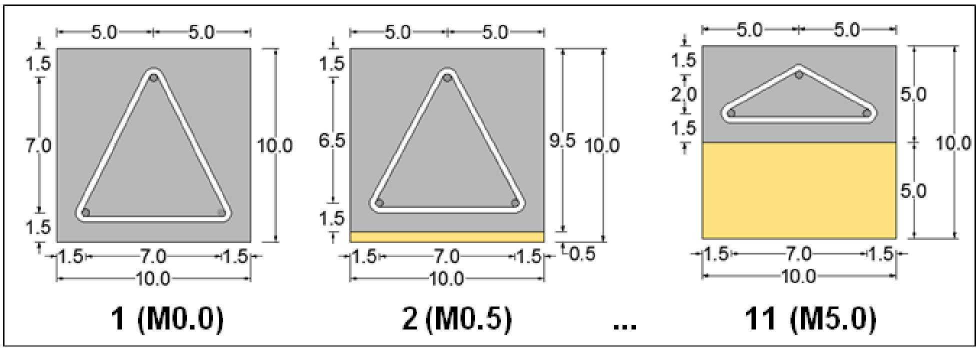

Figure 2. Models cross-sections and notations, measured in cm

The materials models used in the analyses were defined as linear isotropic, their mechanical properties are presented in Table 2.

Table 2. Geometrical and material properties of hybrid lintel components

Component	Cross-section [m]	Density [kg/m^3]	Poisson's ratio	Modulus of elasticity, [GPa]
Concrete	0.10x0.10...0.10x0.05	2300	0.20	30
AAC	0.10x0.005...0.10x0.05	520	0.18	2
Reinforcement	Φ4	7850	0.30	210
Stirrups	Φ3	7850	0.30	210

2.2. Finite element mesh

The meshes were automatically generated and consisted in a number of solid elements varying between 100035 and 110608, associated to 139059 and148950 nodes, as shown in Figure 3.

The finite elements were defined as SOLID185, therefore the mesh consisted in three-dimensional solid elements of 0.0015 - 0.025 m sides, defined by 8 nodes and permitting translations on all three global axes directions.

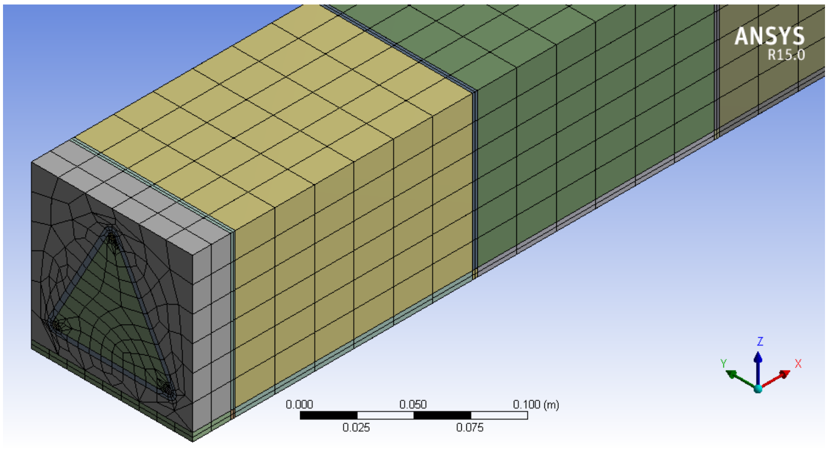

Figure 3. Example of meshing for model number 2

The RC-AAC contact pairs were assigned CONTA174 contact element for the lower part of concrete and TARGE170 target element for the upper part of AAC. Hence, the limits of the deformable bodies were defined using this type of contact pair [8].

2.3. Contact definition

In the case of bonded RC-AAC interface model all connections between the components of the hybrid lintel, steel reinforcement-concrete and AAC-RC are considered perfectly bonded, therefore no separation or detachment may occur between them.

In the case of the frictional RC-AAC interface model, a weak bond between concrete and AAC blocks was assumed by using a friction coefficient of 0.001. Therefore, the contact behaviour is simulated by the Coulomb friction model that also takes into account the shear stresses developed by the two contacting surfaces. This friction model considers that the contact and target surfaces can slide relative to each other. Sliding occurs when shear stresses at interface exceed a certain limit frictional stress, [8]. According to Coulomb friction model and since no cohesion is considered between the two components, the resulted contact frictional stresses are computed by multiplying the friction coefficient with the obtained contact normal pressure.

2.4. Loads and boundary conditions

The loads and boundary conditions are according to serviceability limit state. The lintel has the function to create the needed space for openings of doors and windows and to supports the wall structure placed on it. The maximum deflection of the lintel subjected to transverse loads must be very small, so that not to affect the frames of the openings. The deflection at mid-span was imposed to 1 mm. The applied loads consisted in the automatically generated self-weight of the components and an external load of 1051.8 N, representing three layers of AAC blocks supported by the hybrid element and distributed over the upper surface of the lintel.

The lintel ends were considered fixed, as they are tightly enclosed into the brick wall.

3. NUMERICAL ANALYSIS RESULTS AND DISCUSSION

The results were recorded and analysed in a benchmark for the two contact behaviour approaches. As expected, maximum deflections were obtained at mid-span, while the maximum normal stresses were identified close to the bearing area.

3.1. Normal stresses

All the results regarding normal stresses are introduced in Tables 3, 4 and 5. The results are the extreme values determined in the nodes from the upper and lower edges of the lintel cross-section, both in bearings and mid-span.

When comparing the maximum normal stresses in all lintel components, the highest values were obtained in the concrete layer.

In the case of *bonded models*, in *bearing area*, the tensile stresses in concrete ranged between 2.61 to 5.32 MPa, while the values recorded in the compressed part of the cross-section resulted slightly lower, of -2.63 to -4.23 MPa, see Figure 4.a.

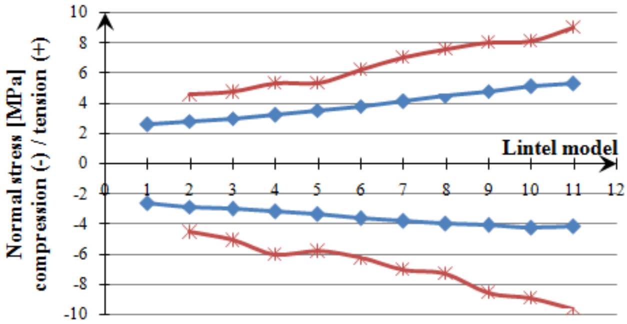

a.

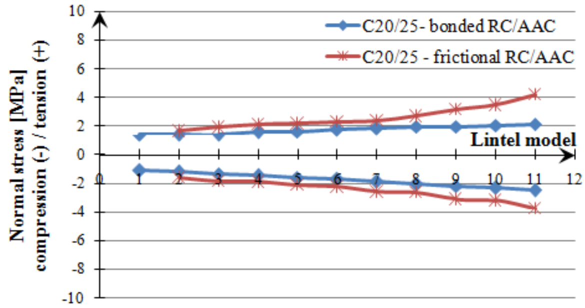

b.

Figure 4. Normal stresses in concrete component for bonded vs. frictional RC/AAC interface: a. results recorded in bearings and b. results recorded at mid-span

The AAC component carries out compression with magnitudes ranging from -0.21 to -0.96 MPa for results recorded in bearings, Fig. 5.a, and tension with magnitudes ranging from 0.10 to 0.40 for results recorded at mid-span.

In the case of bonded models, at *mid-span*, the stresses measured resulted with values of 1.38 to 2.13 MPa at the bottom, and of -1.13 to -2.47 MPa at the upper part of the reinforced concrete cross-section, Fig. 4.b. The stress difference between the tensile and compressed parts of the lintel cross-section at mid-span is also balanced by the stresses developed in the AAC component, which is loaded solely in tension, with values ranging from 0.093 to 0.40 MPa, Fig. 5.b. As expected, due to the bonded interface, the stresses transfer is uniform between components, so that the stress values in the tensile and compressed parts of the cross-section are approximately equal, resulting in a stress difference of only 2.37%.

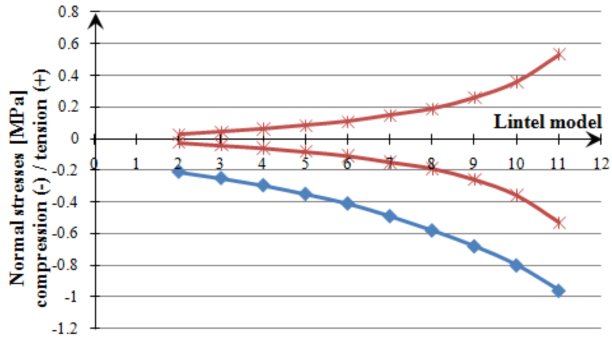

a.

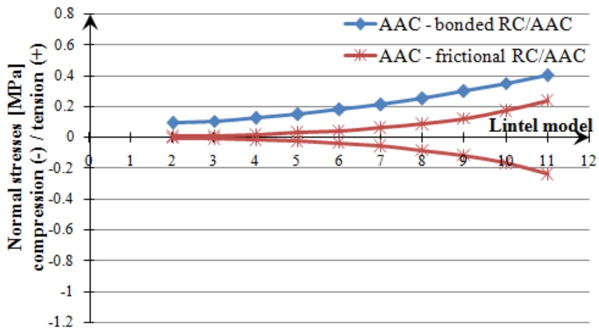

b.

Figure 5. Normal stresses in autoclaved aerated concrete component for bonded vs. frictional RC/AAC interface:
a. results recorded in bearings and b. results recorded at mid-span

Table 3. Normal stresses resulted in concrete

Lintel model	Bonded		Frictional	
	σb bearing [MPa]	σb mid-span [MPa]	σf bearing [MPa]	σf mid-span [MPa]
1	2.61	1.38	-	-
	-2.63	-1.13	-	-
2	2.81	1.42	4.56	1.66
	-2.85	-1.21	-4.54	-1.62
3	3.01	1.38	4.75	1.92
	-2.99	-1.31	-5.08	-1.83
4	3.25	1.57	5.33	2.12
	-3.18	-1.44	-6.03	-1.89
5	3.53	1.61	5.34	2.16
	-3.35	-1.59	-5.82	-2.11
6	3.81	1.72	6.24	2.29
	-3.6	-1.71	-6.27	-2.24
7	4.15	1.86	7.03	2.36
	-3.83	-1.88	-7.04	-2.59
8	4.46	1.96	7.57	2.69
	-3.99	-2.05	-7.29	-2.65
9	4.8	1.97	8.02	3.19
	-4.09	-2.2	-8.57	-3.12
10	5.09	2.06	8.11	3.47
	-4.23	-2.33	-8.89	-3.195
11	5.32	2.13	9	4.18
	-4.16	-2.47	-9.62	-3.75

For the compressed sides of the concrete component, the maximum compressive stresses resulted of -4.16 MPa and are much lower than the compressive strength of concrete, which is 20 MPa, Fig. 6.a. The colour legend suggests that the red areas show where the maximum stresses appear and they get lower towards the green areas.

The normal compression stresses in AAC component measured in bearings vary from -0.21 to -0.96 MPa and do not exceed the compression strength of the material, Table 4. Nevertheless, at mid-span where AAC is only loaded in tension, the tensile strength of AAC is exceeded for models M4.5-6.5[b] and M5-5[b], having the highest value of 0.40 MPa, Fig. 6.b.

Differently from the bonded models, in the *frictional* RC-AAC interface, due to the low bond strength between components, the concrete and AAC carry out stresses individually, both in tension and compression, Figure 7.

Thus, normal stresses in concrete resulted with higher values, both in bearings and at mid-span, varying in *bearings* from 4.56 to 9.00 MPa in tension, and -4.54 to -9.62 in compression, Figure 4.a, and at *mid-span* with values between 1.66 and 4.18 MPa in tension and between -1.62 and -3.75 MPa in compression, Figure 4.b.

Differently from the bonded models, in the *frictional* RC-AAC interface, due to the low bond strength between components, the concrete and AAC carry out stresses individually, both in tension and compression, Figure 7.

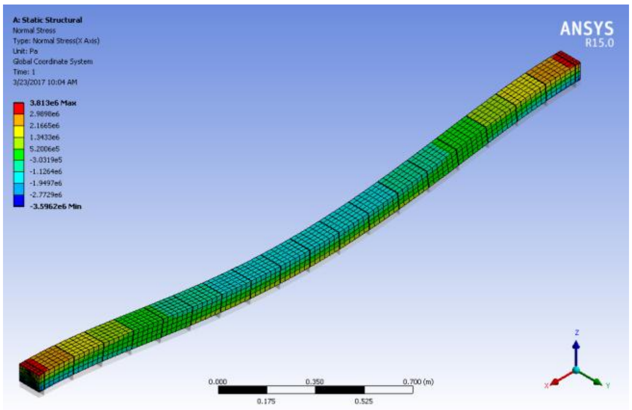

a.

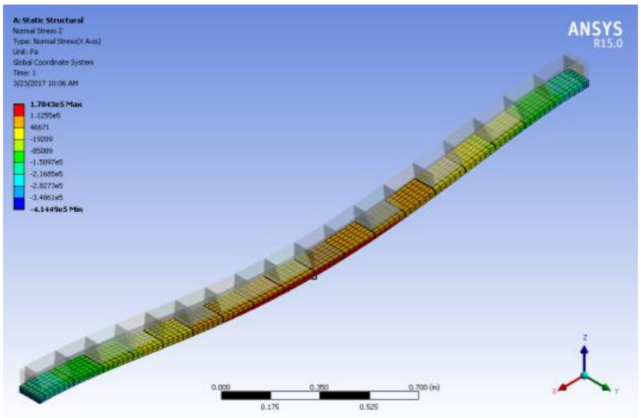

b.

Figure 6. An example of: a. normal stress distribution in concrete and b. in AAC component for bonded contact behaviour

Table 4. Normal stresses resulted in AAC component

Lintel model	Bonded		Frictional	
	σb bearing [MPa]	σb mid-span [MPa]	σf bearing [MPa]	σf mid-span [MPa]
1	-	-	-	-
	-	-	-	-
2	-	0.093	0.027	0.005
	-0.21	-	-0.027	-0.0049
3	-	0.105	0.044	0.011
	-0.25	-	-0.044	-0.011
4	-	0.125	0.062	0.018
	-0.295	-	-0.061	-0.018
5	-	0.15	0.085	0.028
	-0.35	-	-0.084	-0.028
6	-	0.18	0.11	0.041
	-0.41	-	-0.11	-0.041
7	-	0.21	0.15	0.059
	-0.49	-	-0.15	-0.059
8	-	0.25	0.19	0.084
	-0.58	-	-0.19	-0.084
9	-	0.3	0.26	0.12
	-0.68	-	-0.26	-0.12
10	-	0.35	0.36	0.17
	-0.8	-	-0.36	-0.17
11	-	0.4	0.53	0.24
	-0.96	-	-0.53	-0.24

Thus, normal stresses in concrete resulted with higher values, both in bearings and at mid-span, varying in *bearings* from 4.56 to 9.00 MPa in tension, and -4.54 to -9.62 in compression, Figure 4.a, and at *mid-span* with values between 1.66 and 4.18 MPa in tension and between -1.62 and -3.75 MPa in compression, Figure 4.b.

The AAC component presented reduced values for normal stresses at the interface, when compared to those obtained in bonded models, of only 0.027 to 0.53 MPa both in tension and compression in bearings and of 0.005 to 0.24 MPa, both in tension and compression, measured at lintel mid-span, Figure 5.b.

These values are lower than those obtained on bonded models, measured at mid-span, while models M4.5^f and M5.0^f presented tensile stresses in bearings higher than the tensile strength of AAC. This phenomenon occurs due to the lack of interconnection between the components, both being directly influenced by the different modules of elasticity of the materials and to the fact that components deflect differently and leading to a steeper difference between the stresses overtaken by concrete versus AAC.

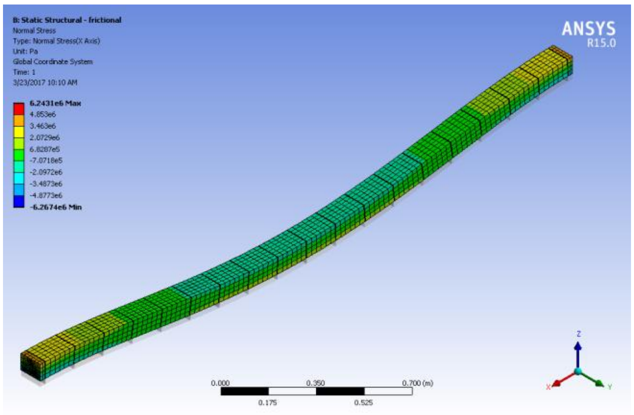

a.

INTERSECTIONS
INTERSECTII
http://www.intersections.ro

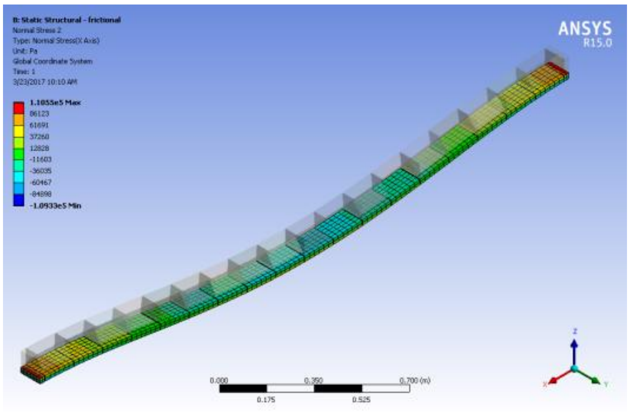

b.

Figure 7. An example of: a. normal stress distribution in concrete and b. in AAC component for frictional contact behaviour

The stresses in steel reinforcement were computed in all three longitudinal bars, and recorded in the upper part of the only longitudinal bar and in the case of the lower part, for the maximum value between both longitudinal bars, Fig. 2. The tensile strength of concrete is exceeded in all models on the upper side of the element and tensile stresses are overtaken instead by the steel reinforcement, Table 5.

The maximum tensile stresses in the steel longitudinal bars are of 25.04 MPa in the case of bonded models and of 26.95 MPa for frictional RC-AAC interface models, and are much lower than the tensile yield strength of 500 MPa, Figure 8.

Table 5. Normal stresses resulted in steel reinforcement

Lintel model	Bonded		Frictional	
	σb bearing [MPa]	σb mid-span [MPa]	σf bearing [MPa]	σf mid-span [MPa]
1	13.85	6.93	-	-
	-13.74	-7.02	-	-
2	15.43	7.721	13.3	6.5
	-14.46	-7.96	-13.37	-6.61
3	16.1	8.29	14.33	6.94
	-15.52	-8.5	-14.25	-7.11
4	16.81	8.43	15.46	7.46
	-15.96	-8.85	-15.3	-7.64
5	18.45	9.08	16.57	8.02
	-17.17	-9.67	-16.36	-8.23
6	19.39	9.7	18.07	8.85
	-18.31	-10.19	-17.72	-9.1
7	20.48	9.58	19.62	9.64

ISSN 1582-3024

Lintel model	Bonded		Frictional	
	σb bearing [MPa]	σb mid-span [MPa]	σf bearing [MPa]	σf mid-span [MPa]
	-18.67	-10.63	-19.13	-9.88
8	22.34	9.77	21.26	10.54
	-19.15	-11.69	-20.67	-10.99
9	23.06	10.03	23.19	11.58
	-19.33	-11.97	-22.13	-11.91
10	24.92	9.37	25.1	12.72
	-18.99	-12.98	-23.49	-13.11
11	25.04	8.69	26.95	13.61
	-17.12	-13.37	-24.64	-14.34

In the *bonded model*, as the two components are not allowed to separate or slide relative to each other, the *interface stresses* are greater than in the case of the frictional contact behaviour models, having values of 0.028 to 0.076 MPa for normal contact stresses and 0.052 to 0.089 MPa for tangential contact stresses, Fig. 9.

In the *frictional model*, the interface stresses resulted with lower values, of 0.006 to 0.028 MPa for normal contact stresses. The tangential contact stresses resulted in 0.1% of the normal contact stresses.

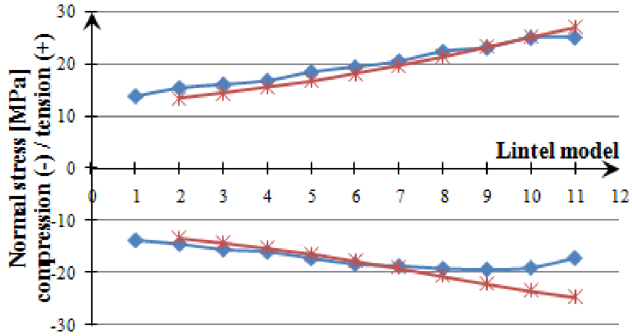

a.

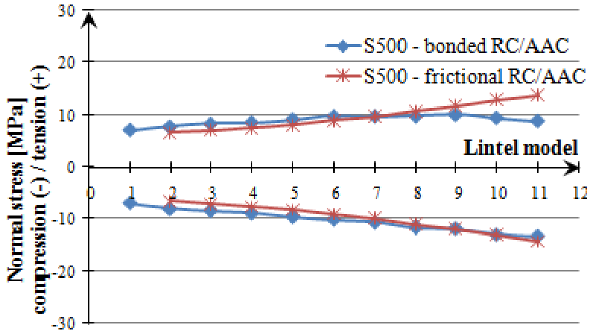

b.

Fig. 8. Normal stresses in steel reinforcement for bonded vs. frictional RC-AAC interface: a. results recorded in bearings and b. results recorded at mid-span

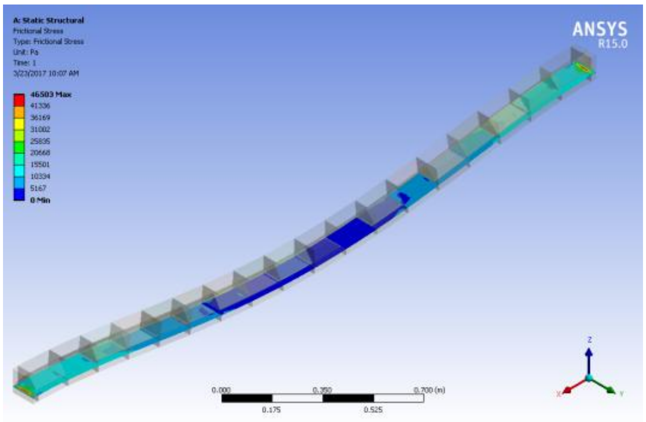

a.

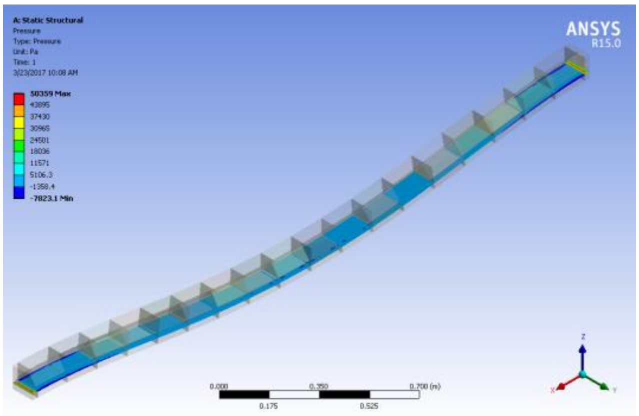

b.

Figure 9. An example of: a. tangential stresses and
b. normal contact stresses at RC-AAC interface for bonded M2.5[b] model

3.2. Maximum deflections

In the *bonded models*, since no discontinuities develop at the RC-AAC interface, the two components deform uniformly, the concrete component restraining the AAC component to deflect differently. The obtained maximum deflection was of 1.35 mm, Fig. 10, and is higher than the allowable deflection, considered of 1 mm, [6, 7].

Otherwise, in the *frictional models*, the maximum deflections measured at the mid-span were varying from 0.4 to 2.27 mm, with up to 40.53% higher than in the case of a perfect bond between the components.

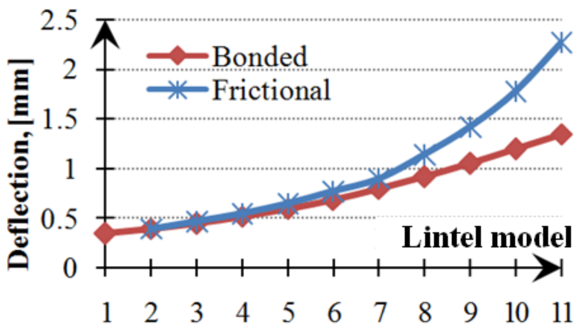

Figure 10. Deflection of lintel measured at mid-span

3.3. Sliding distances and gaps between components

In the *bonded models*, since no discontinuities develop at the RC-AAC interface, the two components deform uniformly, the concrete component restraining the

ISSN 1582-3024

AAC component to deflect differently. The maximum deflection obtained for this analysis was of 1.35 mm, Figure 10, and is higher than the allowable deflection, considered of 1 mm, [6, 7]. In the case of *frictional models*, certain sliding or detachment can occur between RC and AAC layers. Therefore, two effects were analysed at the interface between the concrete and AAC layer: the gap and the sliding distance, Figure 11.a and b.

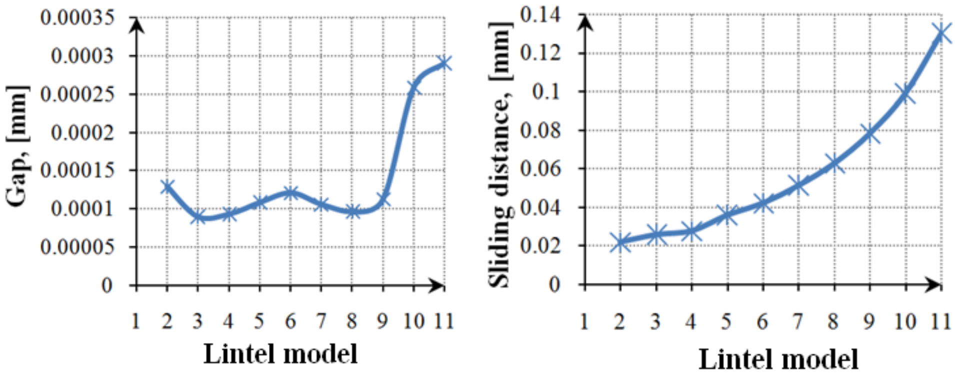

a. b.

Fig. 11. Results obtained for frictional models:
a. gap and b. sliding distance at RC-AAC interface

The gap varies from 0.00013 to 0.00029 mm, presenting an overall increase as the layer of AAC thickens, while the layer of RC is thinner, Fig. 12.a. This appears as a direct consequence of the difference between the stiffness properties of the materials.

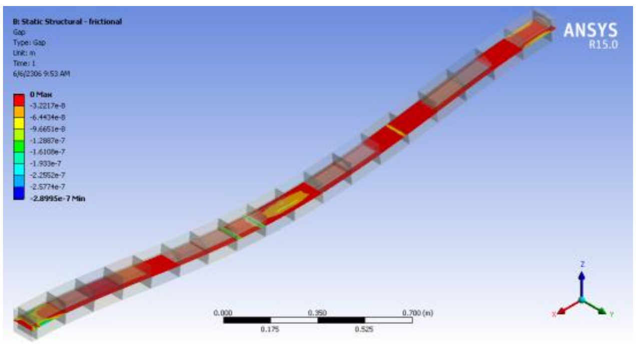

a.

INTERSECTII
INTERSECTIONS
http://www.intersections.ro

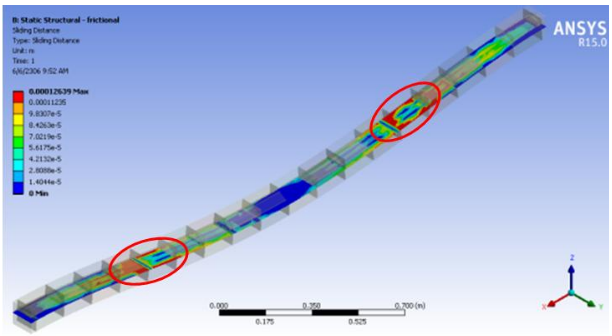

b.

Fig. 12. Example for frictional model M5.0[f] of:
a. gap at RC-AAC interface, b. sliding distance at RC-AAC interface

The sliding distance maps provide a clear view of the most dangerous areas at RC-AAC interface, where sliding may occur. This sliding distance is larger with the increase in AAC component height. The maximum values are obtained in the areas of inflexion, suggested by the red circles in Fig. 12.b. The sliding distance ranges between 0.0222 and 0.13 mm, and it also raises with the increase in AAC height, for the same reasons as the gap, Fig.12.b. These values are only 0.004% for the lintel span, therefore the two components are still working together.

4. FINAL CONCLUSIONS

When selecting the most advantageous configuration for the hybrid lintel, there are certain criteria that must be considered:

- the normal stresses in all components should not exceed the strengths of the individual materials;
- the maximum deflection at mid-span must be lower than the imposed deflection of 1 mm;
- the lowest values for gap and sliding distance at RC-AAC interface are considered the most desirable.

Because all components are subjected to bending, the stresses developed in each of them are both of tension and compression. Since the compressive stresses obtained in all models and in all components do not overcome the compression strength of materials that constitute the lintel, none of bonded and frictional models fail from compressive stresses.

Analysing the AAC layer at mid-span, the last two bonded models (M4.5[b] and M5.0[b]) recorded tensile stresses higher than the AAC tensile strength, considered 10% from its standardised compressive strength of 3.50 MPa. In addition, the AAC components fail in bearing, in the case of the last two frictional models ($M4.5^f$ and $M5.0^f$).

The allowable deflection of 1 mm for the hybrid lintel was exceeded both in bonded and frictional models by the last three ($M4.0^b$, $M4.5^b$, $M5.0^b$) and four models ($M3.5^f$, $M4.0^f$, $M4.5^f$, $M5.0^f$), respectively.

Regarding the gap at the interface for the frictional models, the lower its value, the better the behaviour of the hybrid lintel is considered. Thus, models $M1.0^f$, $M1.5^f$, $M2.0^f$, $M3.0^f$ and $M3.5^f$ present the most advantageous configuration. Nevertheless, $M3.5^f$ does not meet the maximum deflection condition; therefore this configuration should be avoided.

All frictional lintels present very low sliding distances, thus it can be considered that this condition is met by all models.

In conclusion, the configurations that meet all the above-mentioned criteria are M0.5 to M3.0.

In addition, taking into account the fulfilment of the durability requirements and, at the same time, the removal of the thermal bridges and the provision of the thermal transfer resistance of the structural elements in the buildings, the most recommended model is M3.0, meaning that the AAC component should not exceed 30% of the overall cross-section height.

ACKNOWLEDGEMENTS

The authors acknowledge the contribution and thank SC MACON SA Deva which supported the research of these originally products.

This paper was realised in the framework of the project EFECON – ECO-INNOVATIVE PRODUCTS AND TECHNOLOGIES FOR ENERGY EFFICIENCY IN CONSTRUCTION, POC/71/1/4 - Knowledge Transfer Partnership, Cod MySMIS: 105524, ID: P_40_295, Project co-financed by the European Regional Development Fund.

References

1. H. Bagheri, *The BCE (Block Composed Element) building system. A conceptual study*, Licentiate Thesis, Royal Institute of Technology, School of Architecture and Built Environment, Stockholm, ISBN 91-7178-441-1 (2016).
2. B.G. Hellers, O. Lundvall, *Aerated concrete used in composite action with ordinary concrete – from block to element*. Advances in Autoclaved Aerated Concrete, Balkema, Rotterdam, ISBN 90-5410-086-9, pp.201-207 (1992).
3. V. Vimonsatit, A.S. Wahyuni, H. Nikraz, *Reinforced concrete beams with lightweight concrete infill*, Scientific Research and Essays, Vol. 7(27), pp.2370-2379 (2012).

4. T. Subramari, D. Sakthi Kumar, S. Badrinarayanan, *FEM Modelling and Analysis of Reinforced Concrete Section with Light Weight Blocks Infill*, Journal of Engineering Research and Application, Vol. 4, Issue 6, pp.142-149 (2014).
5. Information on http://www.macon.ro.
6. O. Neculai, C. Lanivschi, D.-N. Isopescu, I.-O.Toma, I. Zăpodeanu, *Parametric Study of Structural Performance of Innovative Solutions for Hybrid Lintels* - Part 1: Input Data for FEM Analysis, Advanced Engineering Forum, Trans Tech Publications, Switzerland, Vol. 21, pp. 255-261, ISSN: 2234-991X, doi:10.4028/www.scientific.net/AEF.21.255 (2017).
7. C. Lanivschi, O. Neculai, D.-N. Isopescu, *Structural Behaviour Evaluation by Numerical Simulations for Innovative Solutions of Hybrid Lintels* - Part 2: FEM Analysis, Advanced Engineering Forum, Trans Tech Publications, Switzerland, Vol. 21, pp. 286-293, ISSN: 2234-991X, doi:10.4028/ www.scientific.net/AEF.21.286 (2017).

1. Information on: http://148.204.81.206/Ansys/readme.html.